# UV and IR Absorption Cross-sections of HCHO, HCDO, and DCDO

**Aline Gratien,[†] Elna Nilsson,[‡] Jean-Francois Doussin,[†] Matthew S. Johnson,[‡] Claus J. Nielsen,*[,§] Yngve Stenstrøm,[||] and Bénédicte Picquet-Varrault[†]**

*Laboratoire Interuniversitaire des Systèmes Atmosphériques, UMR 7583, University of Paris 7 and Paris 12, Créteil, France, Copenhagen Center for Atmospheric Research, Department of Chemistry, University of Copenhagen, Universitetsparken 5 DK-2100 Copenhagen OE, Denmark, Centre for Theoretical and Computational Chemistry, Department of Chemistry, University of Oslo, Pb. 1033 − Blindern 0315 Oslo, Norway, and Norwegian University of Life Sciences, Department of Chemistry, Biotechnology and Food Science, Chemistry Section, P.O. Box 5003, N-1432 Aas, Norway*

*Received: June 3, 2007; In Final Form: September 5, 2007*

UV (240−370 nm) and IR (3200−1500 $cm^{-1}$) absorption cross-sections of HCHO, HCDO, and DCDO in a bath gas of $N_2$ at atmospheric pressure and 296 K are reported from simultaneous measurements in the two spectral regions. Cross-sections were placed on an absolute scale through quantitative conversion of formaldehyde to CO and HCOOH by titration with Br atoms, also monitored by FTIR. The integrated UV absorption cross-sections of HCHO, HCDO, and DCDO are equal to within the experimental uncertainty.

## 1. Introduction

Formaldehyde is a key atmospheric trace gas which is formed in the photochemical oxidation of methane and higher hydrocarbons of both natural and anthropogenic origins.[1] Formaldehyde is also emitted by fossil fuel combustion and biomass burning.[2] It plays a key role in atmospheric photochemistry: its photolysis proceeds via two pathways at atmospherically relevant wavelengths and constitutes an important source of $HO_x$ and molecular hydrogen:[3−6]

$$HCHO + h\nu \rightarrow H + HCO \ (\lambda \leq 330 \text{ nm}) \qquad (1a)$$

$$HCHO + h\nu \rightarrow H_2 + CO \ (\lambda \leq 361 \text{ nm}) \qquad (1b)$$

The quantum yield of the two pathways depends on wavelength and thus varies throughout the atmosphere. Under average tropospheric conditions, the two photolysis pathways are of roughly equal importance.[7,8] Formaldehyde therefore plays a significant role in the oxidative capacity of the atmosphere, since it is responsible for a significant fraction of the total $HO_x$ production, particularly in the late morning and afternoon hours.[9] Accurate atmospheric photolysis rates of formaldehyde are required in order to properly model $HO_x$ chemistry.

$H_2$ is an indirect greenhouse gas, since its addition to the atmosphere results in a decrease in the primary atmospheric oxidant OH and a corresponding increase in the greenhouse gas $CH_4$.[10] Several groups have investigated the environmental impact of $H_2$ in the recent past, in part because of the anticipated increase in the use of hydrogen fuel.[11−15] A conversion from a carbon-based to a hydrogen-based economy would have several consequences, including reduced emissions of $NO_x$, VOC, and $CO_2$, lower concentrations of tropospheric ozone, and an increase in stratospheric water vapor.[13] The in situ photolysis of formaldehyde produces over half of the atmosphere's molecular hydrogen. The remaining $H_2$ is due to emissions including biomass burning and fossil fuel combustion.

Analysis of the distribution of stable isotopes in atmospheric species is a promising method for tracking sources and sinks of atmospheric gaseous species.[16−18] Different sources often have different distinguishable isotopic signatures, and the removal processes are likewise associated with distinct fractionations for stable isotopes. In the case of formaldehyde, the loss processes (uptake into droplets, deposition, photolysis, and reaction with radicals) are highly variable, depending on local conditions—the rates of the photolysis and OH processes being approximately equal. We have previously shown that the formaldehyde reactions with OH, Br, Cl, and $NO_3$ radicals exhibit large hydrogen/deuterium kinetic isotope effects (KIEs) ranging from 300‰ for Cl to 7500‰ for Br, whereas the $^{13}C$ KIEs are of the order of −48 (for the OH reaction) to +130‰ (for the Br reaction).[19−21] The deuterium isotope effects in the formation of formaldehyde from methane have been addressed,[22] in addition to the photolytic isotope effects.[23,24] Likewise, the UV spectrum of formaldehyde is modified by isotopic substitution[25] and significant isotope effects in the tropospheric photolysis rates have been demonstrated.[23,26] HCHO photolysis is about 3 times faster than that of DCDO[26] and 1.5 times faster than that of HCDO under tropospheric conditions.[23] Such large isotope effects in photolytic processes immediately raises the question: Are the differences in photolysis rates related to differences in the absorption cross-sections? To answer this, accurate UV cross sections of formaldehyde isotopologues are needed.

In addition to improving our knowledge of its loss processes, accurate measurements of atmospheric HCHO concentrations are required to evaluate its role in $HO_x$ and $H_2$ formation. For this reason, ground-based, air-borne, and balloon-borne or satellite measurements are performed routinely using spectrometers working in the UV and infrared spectral ranges. For example, Differential Optical Absorption Spectroscopy (DOAS) employing the UV spectral region (300−360 nm) is widely used

* To whom correspondence should be addressed: E-Mail: c.j.nielsen@kjemi.uio.no.
[†] Laboratoire Interuniversitaire des Systèmes Atmosphériques.
[‡] University of Copenhagen.
[§] University of Oslo.
[||] Norwegian University of Life Sciences.

10.1021/jp074288r CCC: $37.00 
Published on Web 10/24/2007

in ground-based field measurement of formaldehyde,[27−29] and Chance et al. reported satellite observations of HCHO over North America measured by the GOME instrument aboard the ERS-2 satellite.[30] In the infrared spectral region, formaldehyde concentrations are monitored using the 3.5 $\mu$m (2550−3150 $cm^{-1}$) and the 5−6 $\mu$m (1660−1820 $cm^{-1}$) bands with both Fourier-Transform spectrometers (FTS)[31] and tuneable diode-laser absorption spectrometers (TDLAS).[32,33] In order to obtain accurate concentration profiles, knowledge of the IR and UV absorption cross sections of formaldehyde is therefore of the utmost importance.

The UV absorption cross sections of HCHO have been studied numerous times and critically reviewed.[7] Systematic differences which can reach 20% are observed between several laboratory UV studies commonly used in remote-sensing experiments and photolysis rate calculations.[34−36]

Infrared cross-sections of HCHO are also available for the two bands used to monitor its tropospheric concentrations[37−41] and an IR line list has been deposited in the HITRAN database.[42] However, this list is incomplete and should be used with caution. Moreover, the 5−6 $\mu$m bands (1660−1820 $cm^{-1}$) have been subject to five quantitative spectroscopic studies. Four of the experimental data sets (Nakanaga et al.,[38] Klotz et al.,[39] Sharpe et al.,[40] Herndon et al.[41]) agree with each other to within 5% whereas the very early data of integrated cross-sections by Hisatsune and Eggers[37] are consistently 25% lower.

Concerning DCDO, a quantitative infrared study has been published[38] but no quantitative UV study has been presented. For HCDO there are no equivalent data available.

Recently, we have published an intercomparison of UV (300−360 nm) and infrared (1660−1820 $cm^{-1}$) absorption coefficients of formaldehyde (without determination of absolute absorption coefficients) using simultaneous measurements in both spectral regions.[43] The intercomparison showed good agreement between the UV data published by Meller and Moortgat[34] and a set of four infrared data. In contrast, a rather large discrepancy (about 20%) was observed when using the UV data of Cantrell et al.[35] and Rogers,[36] which are those currently recommended by the HITRAN 2004 database.[42] An absolute intercalibration of UV and IR cross sections is therefore needed to confirm these results. In the present work, we have undertaken a quantitative study of the UV and infrared spectra of formaldehyde isotopologues.

## 2. Experimental Section

The concentration of formaldehyde in spectroscopic cells is inherently difficult to determine accurately by manometric methods because formaldehyde polymerizes and adsorbs on surfaces. Therefore, the determination of UV and infrared cross-sections was performed in two steps: First, infrared cross-sections were determined in the photoreactor in Oslo by quantifying the formaldehyde isotopologue in the cell using titration by bromine atoms (see section 2.1). Second, UV/IR spectra were simultaneously recorded in the LISA photoreactor, and UV cross-sections were deduced from infrared absorption coefficients (section 2.2).

**2.1. Infrared High-Resolution Reference Spectra and Absorption Cross-sections.** The infrared absorption cross-sections were obtained from experiments carried out in a 250 L electropolished stainless steel smog chamber equipped with a White-type multiple reflection mirror system with a 120 m optical path length. The chamber was equipped with UV photolysis lamps mounted in a quartz tube inside the chamber and flushed with air to remove the heat generated. The temperature, monitored on the chamber wall, remained constant for the duration of the experiments. All experiments were carried out in nitrogen atmosphere (AGA, 99.99%) at 296 ± 2 K and 1013 ± 10 hPa. The infrared spectra were recorded with a Bruker IFS 66v FTIR equipped with a liquid nitrogen cooled MCT detector covering the 550−6000 $cm^{-1}$ region. A total of 512 interferograms were co-added, each with a nominal resolution of 0.125 $cm^{-1}$, and transformed using boxcar apodization. The sample was introduced into the chamber by sublimating the respective formaldehyde polymer at 160 °C into a small reservoir on a vacuum line and flushing the gas into the chamber by a stream of nitrogen. The IR and UV spectra did not show evidence for the formation of DCDO or HCHO when the HCDO polymer was heated.

*2.1.1. Titration Procedure*. Before the titration experiments, the cell was cleansed by repeated photolysis of small amounts ozone in 1 atm of air until no formation of $CO/CO_2$ was observed. In the titration experiments, a formaldehyde isotopologue was sublimated and isolated in a bulb on a vacuum line and subsequently flushed into the chamber with nitrogen to a total pressure of 1 atm and a volume fraction of 2−4 ppm. IR spectra were recorded immediately and again after ∼10 min to check that the sample did not adsorb on the cell walls. Around 10% of the gas mixture was then pumped out and 10−15 ppm of $Br_2$ was added in a turbulent stream of air to a final pressure of 1 atm, when a new spectrum of the sample mixture was recorded. Bromine atoms were then generated by photolysis using Philips TLD-08 fluorescence lamps (340−410 nm, $\lambda_{max}$ ∼370 nm) resulting in both ground state, $Br(^2P_{3/2})$, and excited state, $Br(^2P_{1/2})$ (+3685 $cm^{-1}$),[44] atoms.[7] The titration was automated, each cycle consisting of: (1) UV-A photolysis for 15 s and increasing by 15 s each cycle, (2) a waiting period of 30 min, and (3) the recording of two IR spectra.

The experimental infrared spectra were analyzed using a global FTIR nonlinear least-squares spectral fitting procedure, MALT, developed by Griffith.[45] This method simulates the experimental spectrum of the mixture of absorbing species from a set of initial concentrations and reference spectra and then varies the absorber concentrations, the continuum level, and the instrument line-shape parameters, iteratively to minimize the residual between the measured and simulated spectrum. In the spectrum calculation, line parameters from the HITRAN database[42] are used if available, otherwise high-resolution spectra are used.

*2.1.2. High-Resolution Spectra.* High-resolution spectra of the CHDO isotopologue were recorded using a Bruker HR-120 vacuum interferometer and gas cell located at the Maxlab electron storage ring in Lund, Sweden. The experimental system has been described previously[46] and consists of a temperature controlled stainless steel chamber with a volume of 200 L and White-type multipass optics. The distance between the mirrors is 2.85 m, and for these experiments, the system was aligned to give a path length of 11.4 m. A sample of the CHDO polymer was heated to produce the monomer at a pressure of about 6 mbar in a volume of 1.4 L. This sample was flushed into the cell with a small amount of high-purity nitrogen to give a sample pressure in the cell of around 40 $\mu$bar. Depending on the band being examined either an MCT or InSb detector was used, in combination with an appropriate bandpass filter and a globar light source. The CH stretching region of CHDO was recorded at a resolution of 0.0025 $cm^{-1}$, and the CD and CO regions at a resolution of 0.08 $cm^{-1}$. Examples of the obtained data are presented in Figures S1−S3 (see the Supporting Information). The complete spectra are available from the authors upon request.

**2.2. Simultaneous Recording of UV and FTIR Spectra.** The experiments were performed in an evacuable Pyrex photoreactor (6-m long, volume 977 L) at room temperature and atmospheric pressure. A detailed description of this setup is given in Doussin et al.[47] The reactor contains two White-type multiple reflection optical systems interfaced to a Fourier-transform infrared (FTIR) spectrometer and to an UV−vis grating spectrometer.

*2.2.1. UV−vis Measurements.* The system consists of a light source, a beam-splitter, multipass optics inside the reactor, a monochromator, and a CCD camera as detector. The source, the optical parts, and the detector are set on an optical table fixed to the reactor framework and stabilized with rubber shock absorbers. A high-pressure xenon arc lamp (Osram XBO, 450W Xe UV) is used as source in the ultraviolet and visible regions. To reduce stray light in the spectrometer due to the very high intensity of the source in the visible region, a UG5 bandpass filter (Oriel) of 3-mm thickness is permanently placed in the light beam. The UV spectrometer is a Czerny−Turner monochromator with 0.32 m focal length (HR 320, Jobin−Yvon) equipped with a 1200 g $mm^{-1}$ grating and a 1024 × 58 pixel CCD camera (CCD 3000, Jobin-Yvon) as detector. In this configuration, the CCD covers a spectral range of ∼60 nm, and the instrument has a maximum resolution of 0.15 nm. As the formaldehyde absorption covers a rather broad region in the UV (230−360 nm), the experiments were made with three monochromator positions: 240−300 nm, 270−330 nm, and 310−370 nm.

The UV beam is split into two parts: one part enters the optical cell for the measurement, whereas the other one remains outside and is directed to the monochromator to monitor variations in the XBO lamp intensity during the experiment. The absorbance in the UV region is then determined as described in more detail elsewhere.[48]

The wavelength scale of the UV−vis spectrometer was calibrated with reference to 30 emission lines of mercury, zinc, cesium, and cadmium between 240 and 370 nm. The calibration was made in the three regions (240−300, 270−330, and 310−370 nm) used for the acquisition of the spectrum. The UV−vis mirrors of the White cell have aluminum coatings covered with a layer of $AlMgF_2$. The average reflectivity is 83% in the UV region enabling an optimal maximum optical path length of 72 m (base length: 600 ± 1.0 cm). For this study, the optical path length was set to 72.0 m.

*2.2.2. Infrared Measurements.* The infrared spectra were recorded with a Fourier transform spectrometer (BOMEM DA8-ME). The experimental setup comprises a globar light source, a KBr beam splitter, and a liquid nitrogen-cooled MCT detector. This spectrometer allows measurements between 500 and 4000 $cm^{-1}$ with a maximum resolution of 0.013 $cm^{-1}$ (unapodised). The spectrometer is coupled to the reactor multi-reflection White-cell via 0.6° wedged 5-mm thick KBr windows. The mirrors of the cell are "hard" gold-coated and have an average reflectivity of 97%. For the experiments performed in this study, the spectra were recorded with a resolution of 0.1 $cm^{-1}$ and using a boxcar apodization function. The optical path length was set to 12.0 m (base length: 599.7 ± 1.0 cm) to have compatible absorbances in the UV and infrared regions.

*2.2.3. Experimental Procedure.* The procedure followed in each experiment started by pumping the photoreactor to 5 × $10^{-3}$ mbar with irradiation for 1 h. During the experiments, the reactor was filled with pure nitrogen (from liquid nitrogen evaporation, ≥99.995%, Linde) at atmospheric pressure and a temperature of 297 ± 2 K. After the acquisition of infrared and UV reference spectra, HCHO (or DCDO or HCDO) was introduced into the reactor by sublimating approximatly 40 mg (corresponding to about 30 ppm) of paraformaldehyde in a glass tube connected to the chamber and by flushing it into the chamber with dry $N_2$. The UV and infrared absorption spectra of formaldehyde were simultaneously recorded. No impurities or formaldehyde polymers were recorded in either the infrared (IR) or ultraviolet (UV) spectra.

In order to detect possible systematic intensity errors caused by sample and window thermal emissions,[49,50] FTIR spectra with the infrared light source switched off were recorded both with and without formaldehyde in the cell. In all cases, no signal different from noise was detected, indicating that thermal radiation does not lead to systematic infrared absorption errors in the present experimental setup infrared spectral range.

**2.3. Chemicals and Synthesis.** The formaldehyde isotopologues used were in the form of paraformaldehyde, $(CH_2O)_n$. The HCHO sample was a commercial product (Fluka, extra pure); DCDO (CDN, 99.8 D atom%); HCDO was prepared in ∼50% yield by hydrolysis of [2H]-diethoxymethane, $HDC(OEt)_2$, in 30% formic acid at 50 °C under reflux for 1 h using a short Vigreux column and subsequent removal of ethylformate by distillation. The aqueous solution of $HDC(OH)_2$ was then freeze-dried in vacuo to give $(HCDO)_n$. HCOOH was a standard laboratory chemical (Fluka, 99%), DCOOD (Merck, >99 atom% D), was mixed with $H_2O$ to exchange the acidic proton and distilled in vacuo before use. $Br_2$ was a standard laboratory chemical (Fluka, >99%) and distilled in vacuo before use.

[2H]-Diethoxymethane was prepared using a slight modification of a literature procedure.[51] A two-necked round-bottom flask equipped with a condenser and an addition funnel was charged with 5.00 g (119.0 mmol) lithium aluminum deuteride (Fluka, 99.5 atom% D) suspended in 150 mL dry ether and kept under an inert atmosphere ($N_2$). The mass of 11.90 g (80.3 mmol) triethylorthoformate dissolved in 12 mL dry ether was added dropwise to the magnetically stirred suspension over ∼5 min at room temperature. The mixture was refluxed overnight and cooled to room temperature. Ether (25 mL) saturated with water was added dropwise to the vigorously stirred solution followed by 12 mL of 12 M aqueous NaOH. The solution was decanted from the solids thus formed, and the precipitate was washed with ether (3 × 15 mL). The organic phase was collected, dried using $MgSO_4$ and filtered. Ether was carefully distilled using a Vigreux column. Sodium cut in small pieces (1.7 g = 74 mmol) was added to the concentrated solution. The mixture was refluxed for another 3−4 h to remove residual ethanol. Simple distillation gave a crude distillate that was redistilled using a short Vigreux column to give 4.95 g (59%) of the product with a boiling point of 88 °C. NMR spectra of the samples were in accord with the literature.[51]

## 3. Results

**3.1. Infrared Absorption Cross-sections.** The concentrations of formaldehyde in the Oslo photoreactor were determined indirectly by titration with Br atoms—the advantage of using Br instead of Cl atoms is that most other Br atom reactions with organics are endothermic thereby reducing possible systematic errors. For HCHO, the only exothermic reaction in the initial step is as follows:[21]

$$HCHO + Br \rightarrow HCO + HBr \qquad (2)$$

Under atmospheric conditions the formyl radical then reacts with molecular oxygen to give CO and the hydroperxy radical

$$HCO + O_2 \rightarrow CO + HO_2 \quad (3)$$

In a photochemical reactor with ppm concentrations of HCHO, the reversible adduct formation between formaldehyde and the hydroperoxy radical becomes important and cannot be neglected:[52−57]

$$HCHO + HO_2 \rightleftarrows HOO{-}CH_2O \rightleftarrows HO{-}CH_2{-}OO \quad (4)$$

This adduct can react irreversibly in several ways, of which the more important under the present experimental conditions are as follows:[52,54]

$$HO{-}CH_2{-}OO + HO_2 \rightarrow HO{-}CH_2{-}OOH + O_2 \quad (5a)$$

$$\rightarrow HCOOH + O_2 + H_2O \quad (5b)$$

$$2HO{-}CH_2{-}OO \rightarrow HO{-}CH_2{-}OH + HCOOH + O_2 \quad (6a)$$

$$\rightarrow 2HO{-}CH_2{-}O + O_2 \quad (6b)$$

$$HO{-}CH_2{-}O + O_2 \rightarrow HCOOH + HO_2 \quad (7)$$

In an "oxygen-free" atmosphere, however, the dominating processes following the initial hydrogen abstraction will be as follows:[7,58−63]

$$HCO + Br_2 \rightarrow HCOBr + Br \quad (8a)$$

$$\rightarrow CO + HBr + Br \quad (8b)$$

$$HCO + Br \rightarrow CO + HBr \quad (9)$$

$$HCO + HBr \rightarrow HCHO + Br \quad (10)$$

$$HCO + HCO \rightarrow (CHO)_2 \quad (11a)$$

$$\rightarrow HCHO + CO \quad (11b)$$

$$\rightarrow 2CO + H_2 \quad (11c)$$

Glyoxal, should it be formed, will either photolyze very quickly during the photolytic generation of Br atoms, or react very quickly with Br atoms and eventually end up as CO. Formylbromide is thermally unstable and, with a lifetime of ∼10 min in our reactor, it dissociates into CO and HBr, although we cannot exclude that it also reacts with water on the cell walls to form HCOOH and HBr. Thus, in an ideal "oxygen-free" atmosphere, there will be a 1:1 correspondence between formaldehyde used and CO formed in a titration with Br atoms. However, because reaction 3 is quite fast ($5.2 \times 10^{-12}$ cm$^3$ molecule$^{-1}$ s$^{-1}$)[64] even 10 ppm $O_2$ in $N_2$ will make this reaction the dominant loss process for the formyl radical. A FACSIMILE[65] model was written and run to evaluate the importance of reactions 3−11; the rate constants of these reactions are collected in Table S1 (see the Supporting Information). The $O_2$ volume fraction during the titration experiment was estimated from the leakage rate during filling of the reactor to be 10 ppm. Simulations of the HCHO and CO concentrations reproduce the experimental data well. However, it was observed that the HCOOH concentration profiles were very sensitive to $k_{-4}$ ($HO{-}CH_2{-}OO \rightarrow HOO{-}CH_2O \rightarrow HCHO + HO_2$). The literature values for $k_9$[55,57,64,66] span a rather wide range from 23 s$^{-1}$ [57] to 150 s$^{-1}$.[55,66] The best fit to our experimental data was obtained with $k_{-9} = 20$ s$^{-1}$, which is close to the one determined by Zabel et al.,[57] whereas IUPAC[64] recommends the value of Barnes et al.[66] and Veyret et al.[55] Moreover, the simulation confirmed that glyoxal formation (reaction 11a) was a minor process in our conditions, corresponding to approximately 0.01% of reacted formaldehyde.

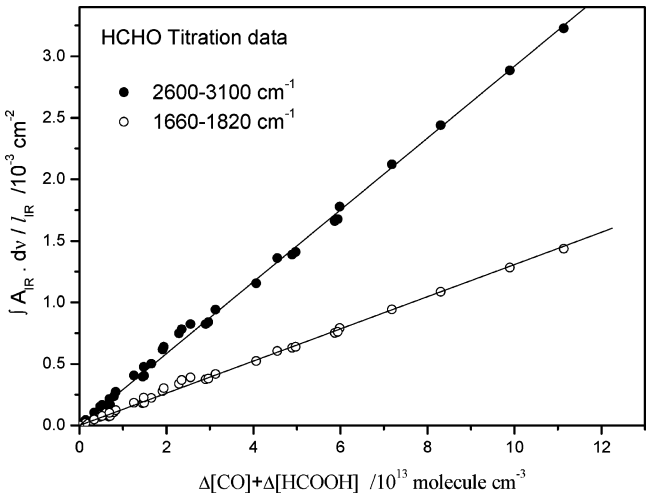


**Figure 1.** Integrated optical depth of HCHO bands during titration with Br atoms. 35 data points from 5 independent experiments give the integrated band intensities $IBI_{(2600-3100cm^{-1})} = (2.92 \pm 0.10) \times 10^{-17}$ cm molecule$^{-1}$ and $IBI_{(1660-1820cm^{-1})} = (1.31 \pm 0.04) \times 10^{-17}$ cm molecule$^{-1}$. The errors quoted take into account the uncertainties in the slopes ($2\sigma$) and those of the CO and HCOOH infrared cross sections.

The spectral features used in the analysis of the formaldehyde removal from the chamber were the C−H stretching bands of HCHO and HCDO in the 3000−2800 cm$^{-1}$ region and the C−D stretching bands of DCDO in the 2300−1900 cm$^{-1}$ region. Experimental high-resolution IR spectra of HCHO, HCDO, and DCDO were used in the analyses. Formic acid was quantified from its strongest band—the $\nu_6(A')$ band at 1105 cm$^{-1}$ (HCOOH) and the $\nu_5(A')$ band at 1142 cm$^{-1}$ (DCOOH); any DCOOD and HCOOD formed from DCDO and HCDO in the titration reactions quickly exchanges the acidic deuterium with water on the reactor surface to end up as DCOOH and HCOOH, respectively. The spectral data needed in the fitting procedure were taken from the HITRAN 2004 database for $H_2O$, CO, and $CO_2$.[42] For HCOOH, the HITRAN 2004 data are incomplete and the cross-section for the $\nu_6(A')$ band is significantly lower than most experimental cross sections.[67−70] In particular, a recent study has shown that HCOOH cross-sections deduced from HITRAN are underestimated by a factor of 2.[71] This new determination, which is in good agreement with most previous experimental ones, was used to quantify formic acid in the present experiments. Reference spectra (4000−550 cm$^{-1}$) of ∼1 ppm HCOOH and DCOOH, respectively, in 1 atm purified air are shown as in transmitance in Figures S4 and S5, respectively (see the Supporting Information). The HCOOH spectrum was quantified from the integrated band intensity of the $\nu_6(A')$ band, $IBI_{(1045-1150\ cm-1)} = 39.2 \times 10^{-18}$ cm molecule$^{-1}$.[71] The DCOOH spectrum was then placed on an absolute scale by comparing the experimental integrated band intensities of the $\nu_1(A')$ bands (the O−H stretching vibrations) in HCOOH and DCOOH spectra with quantum chemical predictions, see Section 3.3.

Table S2 (see the Supporting Information) exemplifies the results from an analysis of the infrared spectra recorded during a titration of HCHO + Br in nitrogen; 90 to 95% of the titrated formaldehyde is converted into CO, whereas 5 to 10% ends up as HCOOH. The infrared spectra, Figure S6 (see the Supporting Information) show that HCOBr—identified by its strongest band, $\nu_2(A')$, at 1798 cm$^{-1}$ and the Fermi-resonance-enhanced $2\nu_6(A')$ overtone band at 1774 cm$^{-1}$—is being formed during the

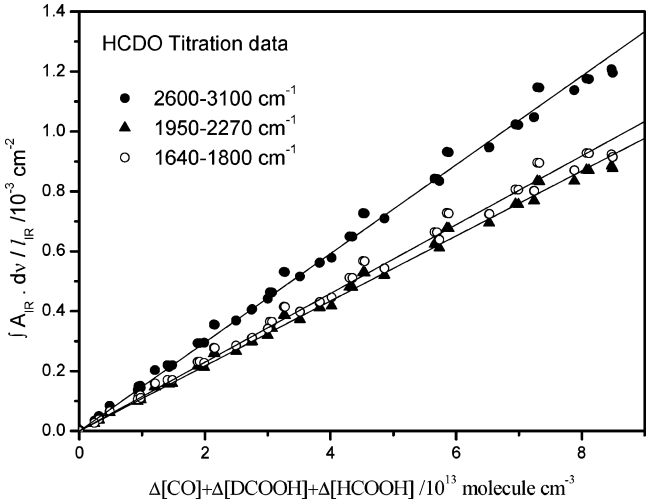


**Figure 2.** Integrated optical depth of HCDO bands during titration with Br atoms. 68 data points from 4 independent experiments give the integrated band intensities $IBI_{(2600-3100cm^{-1})} = (1.48 \pm 0.04) \times 10^{-17}$ cm molecule$^{-1}$, $IBI_{(1950-2270cm^{-1})} = (1.09 \pm 0.04) \times 10^{-17}$ cm molecule$^{-1}$ and $IBI_{(1640-1800cm^{-1})} = (1.15 \pm 0.04) \times 10^{-17}$ cm molecule$^{-1}$. The errors quoted take into account the uncertainties in the slopes ($2\sigma$) and those of CO, HCOOH, and DCOOH infrared cross sections.

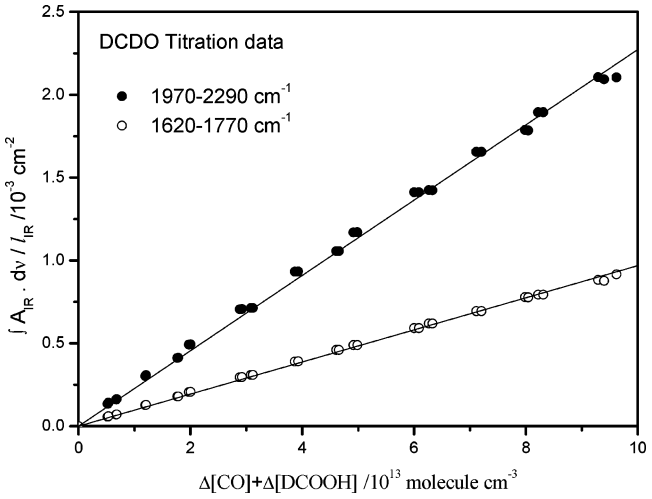


**Figure 3.** Integrated optical depth of DCDO bands during titration with Br atoms. 35 data points from 2 independent experiments give the integrated band intensities $IBI_{(1970-2290cm^{-1})} = (2.27 \pm 0.07) \times 10^{-17}$ cm molecule$^{-1}$ and $IBI_{(1620-1770cm^{-1})} = (0.97 \pm 0.03) \times 10^{-18}$ cm molecule$^{-1}$. The errors quoted take into account the uncertainties in the slopes ($2\sigma$) and those of CO and DCOOH infrared cross sections.

titration.[72] Table S2 also illustrates that small amounts of both CO and HCOOH are formed in the reactor as the bands of HCOBr diminish. A series of 5 titration experiments were carried out for HCHO, whereas 4 experiments were carried out for HCDO and 2 for DCDO. The titration curves are presented in Figures 1−3 from which one may extract the various IBI of HCHO as the slope according to the Beer−Lambert law. The derived average absorption cross sections (base e) are collected in Figure 4, whereas Table 1 compares the IBIs obtained for the three formaldehyde isotopologues with values available in the literature. We note that, at atmospheric pressure, the formaldehyde line-widths in the IR region are about twice the spectral resolution employed.[73] Indicated errors take into account the uncertainties in the slopes ($2\sigma$) and the uncertainties on CO[42] and HCOOH[67−71] infrared cross sections.

**3.2. UV Absorption Cross-sections.** For each formaldehyde isotopomer, several simultaneous recordings of UV (300−360 nm) and IR spectra (900−3300 cm$^{-1}$) were carried out with different formaldehyde concentrations. Infrared spectra were compared to high-resolution spectra acquired in this study to identify potential artifacts (impurities, saturation, and polymerization). Good agreement was observed between the spectra. The quality of the HCHO−UV spectra was checked in our

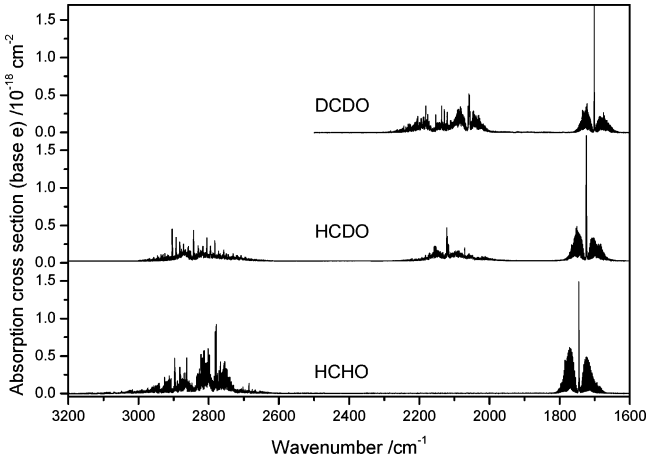


**Figure 4.** Infrared absorption-cross sections of DCDO, HCDO, and HCHO. All spectra were obtained of the samples in nitrogen atmosphere at 296 ± 2 K and 1013 ± 10 hPa.

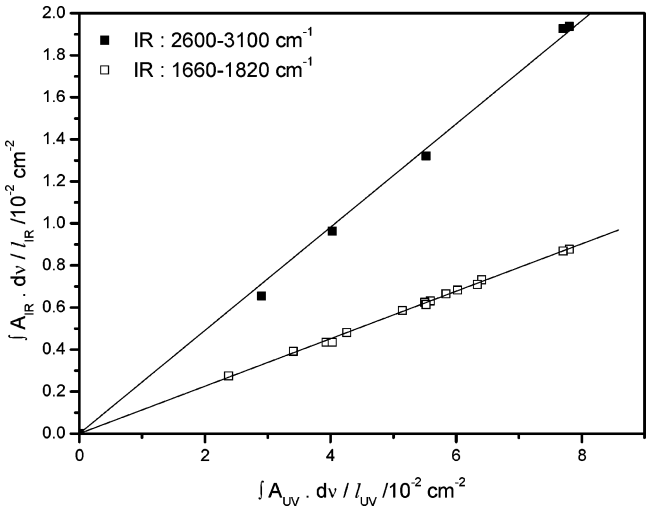


**Figure 5.** IR versus UV integrated optical depths of HCHO. 6 intercomparison experiments give the ratios $IBI_{(2600-3100cm^{-1})}/IBI_{(300-360\ nm)} = 0.246 \pm 0.006$. The errors quoted take into account the uncertainties in the slopes ($2\sigma$). Data from ref 43 give $IBI_{(1660-1820cm^{-1})}/IBI_{(300-360nm)} = 0.113 \pm 0.003$.

**TABLE 1: Integrated Band Intensities, IBI, of HCHO, HCDO, and DCDO in the Infrared Region**

| molecule | spectral range /cm$^{-1}$ | this work /$10^{-17}$ cm$^{-1}$ | literature values /$10^{-17}$ cm$^{-1}$ |
|---|---|---|---|
| HCHO | 2600−3100 | 2.92 ± 0.10 | 2.126 ± 0.914 [37] |
| | | | 2.708 ± 0.099 [38] |
| | | | 2.800 ± 0.140 [40] |
| | 1660−1820 | 1.31 ± 0.04 | 0.963 ± 0.199 [37] |
| | | | 1.229 ± 0.040 [38] |
| | | | 1.262 ± 0.083 [41] |
| | | | 1.248 ± 0.126 [39] |
| | | | 1.284 ± 0.064 [40] |
| HCDO | 2600−3100 | 1.48 ± 0.04 | |
| | 1950−2270 | 1.09 ± 0.04 | |
| | 1640−1800 | 1.15 ± 0.04 | |
| DCDO | 1970−2290 | 2.27 ± 0.07 | 2.138 ± 0.068 [38] |
| | 1620−1770 | 0.97 ± 0.03 | 0.882 ± 0.028 [38] |

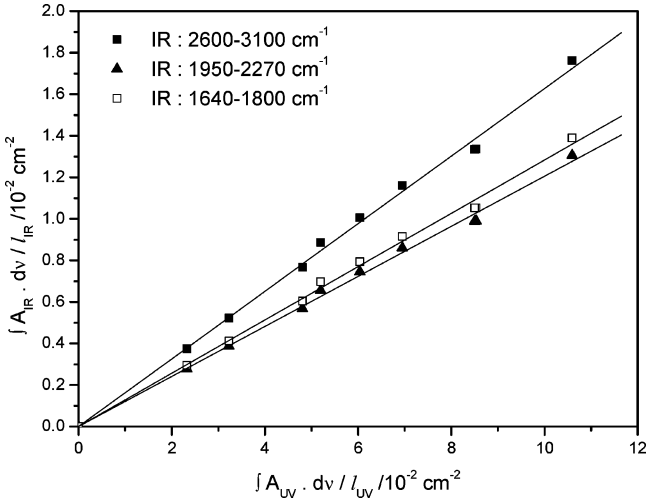


**Figure 6.** IR and UV integrated optical depths of HCDO. 10 intercomparison experiments were performed by simultaneously acquiring UV and IR spectra and give the ratios. $IBI_{(2600-3100cm^{-1})}/IBI_{(300-360nm)} = 0.163 \pm 0.003$, $IBI_{(1950-2270cm^{-1})}/IBI_{(300-360nm)} = 0.120 \pm 0.002$ and $IBI_{(1640-1800cm^{-1})}/IBI_{(300-360nm)} = 0.128 \pm 0.002$. The errors quoted take into account the uncertainties in the slopes ($2\sigma$).

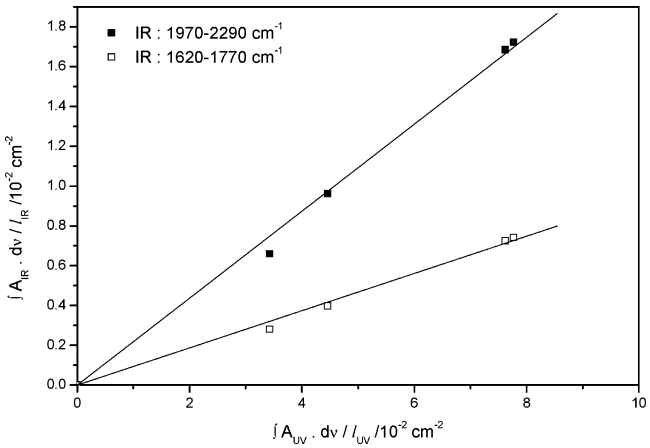


**Figure 7.** IR and UV integrated optical depths of DCDO. 5 intercomparison experiments were performed by simultaneously acquiring UV and IR spectra and give the ratios. $IBI_{(1970-2290cm^{-1})}/IBI_{(300-360nm)} = 0.218 \pm 0.011$ and $IBI_{(1620-1770cm^{-1})}/IBI_{(300-360nm)} = 0.093 \pm 0.006$. The errors quoted take into account the uncertainties in the slopes ($2\sigma$).

previous study;[43] we expect a similar quality of the DCDO and HCDO UV spectra.

The quantities $\int A_{IR}(\tilde{\nu})\, d\tilde{\nu}/l_{IR}$ and $\int A_{UV}(\tilde{\nu})\, d\tilde{\nu}/l_{UV}$, in which $l_{IR}$ and $l_{UV}$ are the optical path lengths of the IR and UV beams, respectively, were calculated for the various experiments. In the IR region, the measured absorbance of HCHO was integrated over the regions 1660−1820 and 2600−3100 $cm^{-1}$; for DCDO, the integration regions were 1970−2290 and 1620−1770 $cm^{-1}$; and for HCDO, the regions 1640−1800, 1950−2270, and 2600−3100 $cm^{-1}$ were employed. In the UV region, integrations were performed over the region from 300 to 360 nm (27778 to 33333 $cm^{-1}$) for the three isotopologues. Figures 5−7 show plots of $\int A_{IR}(\tilde{\nu})\, d\tilde{\nu}/l_{IR}$ for various bands versus $\int A_{UV}(\tilde{\nu})\, d\tilde{\nu}/l_{UV}$ for HCHO, HCDO and DCDO, respectively. According to the Beer−Lambert law, the slopes of the straight lines fitted to the data correspond to the ratios $IBI_{IR}/IBI_{UV}$. The internal consistency of the data of the present study is very good, showing that the linearity of absorption is clearly fulfilled.

The ratios of $IBI_{IR}/IBI_{UV}$ obtained in this work are presented in Table 2. The errors given take into account the uncertainties in the slopes ($2\sigma$) as well as systematic errors (paths lengths,

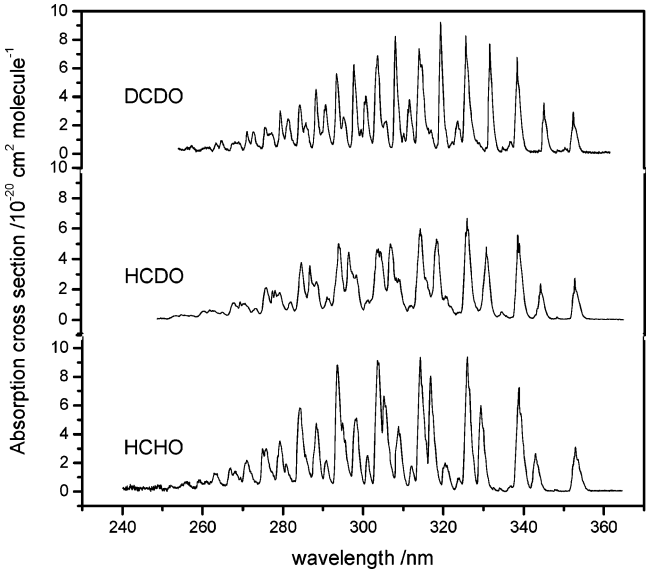


**Figure 8.** Ultraviolet absorption-cross sections of DCDO, HCDO, and HCHO (resolution: 0.18 nm).

**TABLE 2: Ratios $IBI_{IR}/IBI_{UV(300-360nm)}$ of HCHO, HCDO, and DCDO Deduced from IR/UV Intercomparison Experiments**

| IR spectral range ($cm^{-1}$) | HCHO | HCDO | DCDO |
|---|---|---|---|
| 2600−3100 | $0.246 \pm 0.006$ | $0.163 \pm 0.003$ | |
| 1640−1800 | $0.113 \pm 0.003$[a] | $0.128 \pm 0.002$ | |
| 1950−2270 | | $0.120 \pm 0.002$ | |
| 1620−1770 | | | $0.093 \pm 0.006$ |
| 1970−2290 | | | $0.218 \pm 0.011$ |

[a] Data for the 1660−1820 $cm^{-1}$ region from ref 43.

**TABLE 3: Integrated Band Intensities (/$10^{-16}$ cm $molecule^{-1}$) in the 300−360 nm UV-region of HCHO, HCDO, and DCDO**

| | this work | Meller and Moortgat[34] | Cantrell et al.[35] | Rogers[36] |
|---|---|---|---|---|
| HCHO | $1.172 \pm 0.066$ | $1.110 \pm 0.055$ | $0.934 \pm 0.093$ | $0.950 \pm 0.019$ |
| HCDO | $0.932 \pm 0.051$ | | | |
| DCDO | $1.042 \pm 0.089$ | | | |

stray light). The UV absorption cross-sections of the formaldehyde isotopologues shown in Figure 8 were then derived from these ratios and from the infrared cross sections obtained in section 3.2. Table S3 (see the Supporting Information) lists the absorption cross-sections averaged over 1-nm intervals. The UV spectra were obtained with a spectral resolution of 0.18 nm. Consequently, true peak absorption cross-sections are underestimated because the spectrometer resolution is much less than the rotational line widths, and only the integrated absorption cross-sections of HCHO, HCDO, and DCDO in the 300−360 nm region are compared with previous results in Table 3. The errors quoted take into account the uncertainties from the ratios $IBI_{IR}/IBI_{UV}$ and from the infrared cross sections. To compare the spectra of HCHO from the present study with the recent quantitative high-resolution UV data,[74−76] a band-by-band comparison of integrated intensities for the main vibronic bands in the 300−360 nm regions of HCHO is presented in Table 4.

**3.3. Quantum Chemical Calculations.** Quantum chemical DFT (B3LYP) calculations were performed with Gaussian 03[77] employing the cc-pVTZ, aug-cc-pVTZ, cc-pVQZ, and cc-pV5Z basis sets. The equilibrium geometries and the normal modes of HCOOH and DCOOH, including infrared intensities, were calculated with all four basis sets. In addition, the anharmonic

**TABLE 4: Integrated Band Intensities (/$10^{-17}$ cm molecule$^{-1}$) for the Main Vibronic Bands in the 300−360 nm UV-Region of HCHO**

| UV spectral range (nm) | this work | Meller and Moortgat [34] | Cantrell et al. [35] | Rogers [36] | Smith et al.[76] | Pope et al.[74] | Co et al.[75] |
|---|---|---|---|---|---|---|---|
| 302.8−305. 1 | 1.38 ± 0.04 | 1.308 | 1.227 | 1.22 | 1.359 ± 0.022 | | |
| 305.1−308. 2 | 1.08 ± 0.07 | 1.000 | 0.918 | 0.93 | 1.140 ± 0.028 | | |
| 308.2−311. 3 | 0.70 ± 0.04 | 0.655 | 0.649 | 0.65 | 0.724 ± 0.004 | | |
| 313.5−316. 5 | 1.40 ± 0.09 | 1.371 | 1.324 | 1.28 | 1.396 ± 0.010 | 1.43 | |
| 316.5−319. 7 | 1.14 ± 0.06 | 1.022 | 0.976 | 0.94 | 1.122 ± 0.053 | 1.15 | |
| 325.2−328. 7 | 1.27 ± 0.08 | 1.278 | 1.291 | 1.25 | 1.285 ± 0.010 | | |
| 328.7−332. 8 | 0.82 ± 0.05 | 0.804 | 0.791 | 0.75 | 0.842 ± 0.006 | | |
| 337.7−340. 1 | 0.79 ± 0.04 | 0.803 | 0.821 | 0.80 | 0.756 ± 0.094 | | |
| 351.7−355. 5 | 0.44 ± 0.03 | 0.424 | 0.367 | 0.37 | | | 0.411 |

force field of formic acid was calculated at the B3LYP/cc-pVTZ level. The calculated normal modes of vibration including their infrared intensities are summarized in Table S4 (see the Supporting Information). The main result pertaining to the present work concerns the infrared intensities of the two isotopologues. The calculations show that the OH-stretching modes in HCOOH and DCOOH essentially have the same integrated band intensity. This result can be used to place the infrared absorption cross-sections of DCOOH on an absolute scale once the infrared absorption cross-sections of HCOOH are known.

## 4. Discussion

The following conclusions can be made based on the results shown in Table 1: The present integrated infrared band intensities of HCHO are in agreement with the literature[38−41] when the appropriate experimental uncertainties are taken into account. We note that the recommended intensities found in HITRAN 2004 are not in agreement with the available body of measurements. The infrared integrated band intensities of DCDO are in agreement with the literature by considering the uncertainties for the regions 1970−2290 cm$^{-1}$ but are in disagreement by about 9% for the 1950−2290 cm$^{-1}$ region.

In the UV region, the present IBIs for the region 300−360 nm compare well (about 5% difference) with the data of Meller and Moortgat.[34] Looking at the band by band IBIs collected in Table 4, the discrepancy varies from 2% to 11% depending on the band considered. Furthermore, it can be seen from Table 4 that our results are in excellent agreement (better than 2%) with the high-resolution data published by Smith et al.[76] and Pope et al.[74] The data of Co et al.[75] are about 7% lower for the band 351.7−355.5 nm than our results, but consistent when taking into account the uncertainties. Finally, the consistency between the data of Smith et al.[76] and the present ones suggest that the Meller and Moortgat[34] data are slightly too low by about 5%.

In contrast, a difference of about 20% is observed when comparing with the UV cross-sections published by Cantrell et al.[35] and by Rogers.[36] This is also in agreement with our recent study on formaldehyde.[43] In summary, all recent studies on the UV cross sections of HCHO suggest that the data in the HITRAN database,[78] which are based on the data of Cantrell et al.,[35] are too low by around 20%.

The improved cross-sections calibrated using quantitative conversion to CO and HCOOH combined with simultaneous measurement of the IR and UV cross sections of the formaldehyde isotopomers will help in experiments using spectroscopic data, including remote sensing and laboratory kinetics. Formaldehyde is a key reactive intermediate and its deuterium enrichment has recently been shown to vary from −296 to +210 per mil in atmospheric samples.[79] Further study is needed in order to associate these variations with atmospheric photochemistry and specific emissions sources.

The experiments demonstrate that the integrated UV absorption cross-sections of HCHO, HCDO, and DCDO are equal to within the experimental uncertainty. Therefore, the differences in photolysis rates and branching ratios for the molecular and radical channels for the H isotopologues[23,24] must be due to dynamics,[80] and not differing absorption rates.

**Acknowledgment.** This work is part of the ACTION project supported by the Norwegian Research Council under contracts 155959/S30 and 160270/V30. The Norwegian High Performance Computing Consortium is acknowledged for grants of computing time. M.S.J. and E.N. thank the Copenhagen Center for Atmospheric Research supported by the Danish Natural Science Research Council and the Villum Kahn Rasmussen Fund. Financial support from the French National Program of Atmospheric Chemistry is acknowledged.

**Supporting Information Available:** Reactions and rate coefficients used in FACSIMILE modeling of the Br-titration of formaldehyde (Table S1). Example of results from HCHO + Br titration monitored by FTIR (Table S2). UV absorption cross sections of HCHO, DCDO, and HCDO averaged over 1 nm intervals (Table S3). Vibrational frequencies and infrared intensities of HCOOH and DCOOH from quantum chemical calculations (Table S4). Cut of the high-resolution CH stretching band of HCDO (Figure S1). Cut of the high-resolution CO stretching of HCDO (Figure S2). Cut of the high-resolution CD stretching band of HCDO (Figure S3). Infrared vapor-phase spectrum of HCOOH (Figure S4). Infrared vapor-phase spectrum of DCOOH (Figure S5). Infrared spectra of the carbonyl stretching region during a HCHO + Br titration (Figure S6). This material is available free of charge via the Internet at http://pubs.acs.org.

## References and Notes

(1) Anderson, L. G.; Lanning, J. A.; Barrell, R.; Miyagishima, J.; Jones, R. H.; Wolfe, P. *Atmos. Environ.* **1996**, *30*, 2113.

(2) Carlier, P.; Hannachi, H.; Mouvier, G. *Atmos. Environ.* **1986**, *20*, 2079.

(3) Novelli, P. C.; Lang, P. M.; Masarie, K. A.; Hurst, D. F.; Myers, R.; Elkins, J. W. *J. Geophys. Res.—Atmos.* **1999**, *104*, 30427.

(4) Sanderson, M. G.; Collins, W. J.; Derwent, R. G.; Johnson, C. E. *J. Atmos. Chem.* **2003**, *46*, 15.

(5) Seiler, W.; Conrad, R. Contribution of tropical ecosystems to the global budgets of trace gases, especially $CH_4$, $H_2$, CO, and $N_2O$. In *The Geophysiology of Amazonia*; Dickinson, R. E., Ed.; John Wiley and Sons: New York 1987; pp 133.

(6) Warneck, P. *Chemistry of the Natural Atmosphere*, 2nd ed.; Academic Press: New York 1999.

(7) Sander, S. P.; Golden, D. M.; Kurylo, M. J.; Moortgat, G. K.; Wine, P. H.; Ravishankara, A. R.; Kolb, C. E.; Molina, M. J.; Finlayson-Pitts, B. J.; Huie, R. E.; Orkin, V. L. "Chemical Kinetics and Photochemical Data for Use in Atmospheric Studies. Evaluation Number 15," National Aeronautics and Space Administration, Jet Propulsion Laboratory, California Institute of Technology, 2006.

(8) Smith, G. D.; Molina, L. T.; Molina, M. J. *J. Phys. Chem. A* **2002**, *106*, 1233.

(9) Fried, A.; McKeen, S.; Sewell, S.; Harder, J.; Henry, B.; Goldan, P.; Kuster, W.; Williams, E.; Baumann, K.; Shetter, R.; Cantrell, C. *J. Geophys. Res.* **1997**, *102*, 6283.
(10) IPCC "Climate Change 2001: The Scientific Basis. Contribution of Working Group I to the Third Assessment Report of the Intergovernmental Panel on Climate Change," Cambridge University Press, 2001.
(11) Hauglustaine, D. A.; Ehhalt, D. H. *J. Geophys. Res.—Atmos.* **2002**, *107*.
(12) Rahn, T.; Eiler, J. M.; Kitchen, N.; Fessenden, J. E.; Randerson, J. T. *Geophys. Res. Lett.* **2002**, *29*.
(13) Schultz, M. G.; Diehl, T.; Brasseur, G. P.; Zittel, W. *Science* **2003**, *302*, 624.
(14) Tromp, T. K.; Shia, R. L.; Allen, M.; Eiler, J. M.; Yung, Y. L. *Science* **2003**, *300*, 1740.
(15) Warwick, N. J.; Bekki, S.; Nisbet, E. G.; Pyle, J. A. *Geophys. Res. Lett.* **2004**, *31*.
(16) Brenninkmeijer, C. A. M.; Janssen, C.; Kaiser, J.; Röckmann, T.; Rhee, T. S.; Assonov, S. S. *Chem. Rev.* **2003**, *103*, 5125.
(17) Goldstein, A. H.; Shaw, S. L. *Chem. Rev.* **2003**, *103*, 5025.
(18) Johnson, M. S.; Feilberg, K. L.; von Hessberg, P.; Nielsen, O. J. *Chem. Soc. Rev.* **2002**, *31*, 313.
(19) Feilberg, K. L.; Johnson, M. S.; Nielsen, C. J. *J. Phys. Chem.* A **2004**, *108*, 7393.
(20) D'Anna, B.; Bakken, V.; Beukes, J. A.; Nielsen, C. J.; Brudnik, K.; Jodkowski, J. T. *Phys. Chem. Chem. Phys.* **2003**, *5*, 1790.
(21) Beukes, J. A.; D'Anna, B.; Bakken, V.; Nielsen, C. J. *Phys. Chem. Chem. Phys.* **2000**, *2*, 4049.
(22) Nilsson, E.; Johnson, M. S.; Taketani, F.; Matsumi, Y.; Hurley, M. D.; Wallington, T. J. *Atmos. Chem. Phys. Discuss.* **2007**, *7*, 10019.
(23) Feilberg, K. L.; Johnson, M. S.; Bacak, A.; Röckmann, T.; Nielsen, C. J. *J. Phys. Chem. A* **2007**, *111*, 9034.
(24) Rhee, T. S.; Brenninkmeijer, C. A. M.; Röckmann, T. *Atmos. Chem. Phys. Discuss.* **2007**, *7*, 12715.
(25) Miller, R. G. Photophysics of single vibronic levels in the $\tilde{A}^1A_2$ state of $H_2CO$, HDCO, and $D_2CO$, Dissertation, University of California, Irvine, 1975.
(26) Feilberg, K. L.; D'Anna, B.; Johnson, M. S.; Nielsen, C. J. *J. Phys. Chem.* A **2005**, *109*, 8314.
(27) Grutter, M.; Flores, E.; Andraca-Ayala, G.; Baez, A. *Atmos. Environ.* **2005**, *39*, 1027−1034.
(28) Heckel, A.; Richter, A.; Tarsu, T.; Wittrock, F.; Hak, C.; Pundt, I.; Junkermann, W.; Burrows, J. P. *Atmos. Chem. Phys.* **2005**, *5*, 909.
(29) Platt, U.; Perner, D. *J. Geophys. Res.* **1980**, *85*, 7453.
(30) Chance, K.; Palmer, P. I.; Spurr, R. J. D.; Martin, R. V.; Kurosu, T. P.; Jacob, D. J. *Geophys. Res. Lett.* **2000**, *27*, 3461.
(31) Yokelson, R. J.; Goode, J. G.; Ward, D. E.; Susott, R. A.; Babbitt, R. E.; Wade, D. D.; Bertschi, I.; Griffith, D. W. T.; Hao, W. M. *J. Geophys. Res.* **1999**, *104*, 30109.
(32) Fried, A.; Wert, B. P.; Henry, B.; Drummond, J. R. *Spectrochim. Acta Part A* **1999**, *55*, 2097.
(33) Wagner, G.; Schiller, C.; Fischer, H. *J. Geophys. Res.* **2001**, *106*, 28529.
(34) Meller, R.; Moortgat, G. K. *J. Geophys. Res.* **2000**, *105*, 7089.
(35) Cantrell, C. A.; Davidson, J. A.; McDaniel, A. H.; Shetter, R. E.; Calvert, J. G. *J. Phys. Chem.* **1990**, *94*, 3902.
(36) Rogers, J. D. *J. Phys. Chem.* **1990**, *94*, 4011.
(37) Hisatsune, C.; Eggers, D. F. *J. Chem. Phys.* **1955**, *23*, 487.
(38) Nakanaga, T.; Kondo, S.; Saëki, S. *J. Chem. Phys.* **1982**, *76*, 3860.
(39) Klotz, B.; Barnes, I.; Imamura, T. *Phys. Chem. Chem. Phys.* **2004**, *6*, 1725.
(40) Sharpe, S. W.; Johnson, T. J.; Sams, R. L.; Chu, P. M.; Rhoderick, G. C.; Johnson, P. A. *Appl. Spectrosc.* **2004**, *58*, 1452.
(41) Herndon, S. C.; Nelson, D. D. J.; Li, Y.; Zahniser, M. S. *J. Quant. Spectrosc. Radiat. Transfer* **2005**, *90*, 207.
(42) Rothman, L. S.; Jacquemart, D.; Barbe, A.; Benner, D. C.; Birk, M.; Brown, L. R.; Carleer, M. R.; Chackerian, C.; Chance, K.; Coudert, L. H.; Dana, V.; Devi, V. M.; Flaud, J. M.; Gamache, R. R.; Goldman, A.; Hartmann, J. M.; Jucks, K. W.; Maki, A. G.; Mandin, J. Y.; Massie, S. T.; Orphal, J.; Perrin, A.; Rinsland, C. P.; Smith, M. A. H.; Tennyson, J.; Tolchenov, R. N.; Toth, R. A.; Vander Auwera, J.; Varanasi, P.; Wagner, G. *J. Quant. Spectrosc. Radiat. Transfer* **2005**, *96*, 139.
(43) Gratien, A.; Picquet-Varrault, B.; Orphal, J.; Perraudin, E.; Doussin, J. F.; Flaud, J.-M. *J. Geophys.l Res.* **2007**, *112*, *D05305*, *doi:10.1029/2006JD007201*.
(44) Kelly, R. L. *J. Phys. Chem. Ref. Data*, Supplement **1987**, *16*, 1371.
(45) Griffith, D. W. T. *Appl. Spectrosc.* **1996**, *50*, 59.
(46) Johnson, M. S.; Hegelund, F.; Nelander, B. *J. Mol. Spectrosc.* **1998**, *190*, 269.
(47) Doussin, J. F.; Ritz, D.; Durand-Jolibois, R.; Monod, A.; Carlier, P. *Analysis 2* **1997**, *25*, 236.
(48) Picquet-Varrault, B.; Orphal, J.; Doussin, J. F.; Carlier, P.; Flaud, J.-M. *J. Atmos. Chem. A.* **2005**, *109*, 1008.
(49) Birk, M.; Hausamann, D.; Wagner, G.; Johns, J. W. *Appl. Phys. B* **1996**, *35*, 2971.
(50) Ballard, J.; Remedios, J. J.; Roscoe, H. K. *J. Quant. Spectrosc. Radiat. Transfer* **1992**, *48*, 733.
(51) Hanley, J. A.; Forsyth, D. A. *J. Labelled Compd. Radiopharm.* **1990**, *28*, 307.
(52) Su, F.; Calvert, J. G.; Shaw, J. H. *J. Phys. Chem.* **1979**, *83*, 3185.
(53) Su, F.; Calvert, J. G.; Shaw, J. H.; Niki, H.; Maker, P. D.; Savage, C. M.; Breitenbach, L. D. *Chem. Phys. Lett.* **1979**, *65*, 221.
(54) Burrows, J. P.; Moortgat, G. K.; Tyndall, G. S.; Cox, R. A.; Jenkin, M. E.; Hayman, G. D.; Veyret, B. *J. Phys. Chem.* **1989**, *93*, 2375.
(55) Veyret, B.; Lesclaux, R.; Rayez, M. T.; Rayez, J. C.; Cox, R. A.; Moortgat, G. K. *J. Phys. Chem.* **1989**, *93*, 2368.
(56) Veyret, B.; Rayez, J. C.; Lesclaux, R. *J. Phys. Chem.* **1982**, *86*, 3424.
(57) Zabel, F.; Sahetchian, K. A.; Chachaty, C. *Chem. Phys. Lett.* **1987**, *134*, 433.
(58) Poulet, G.; Laverdet, G.; Lebras, G. *J. Chem. Phys.* **1984**, *80*, 1922.
(59) Becerra, R.; Carpenter, I. W.; Walsh, R. *J. Phys. Chem.* A **1997**, *101*, 4185.
(60) Timonen, R. S.; Ratajczak, E.; Gutman, D. *J. Phys. Chem.* **1988**, *92*, 651.
(61) Quee, M. J. Y.; Thynne, J. C. J. *Ber. Bunsen-Ges. Phys. Chem.* **1968**, *72*, 211.
(62) Stoeckel, F.; Schuh, M. D.; Goldstein, N.; Atkinson, G. H. *Chem. Phys.* **1985**, *95*, 135.
(63) Friedrichs, G.; Herbon, J. T.; Davidson, D. F.; Hanson, R. K. *Phys. Chem. Chem. Phys.* **2002**, *4*, 5778.
(64) Atkinson, R.; Baulch, D. L.; Cox, R. A.; Crowley, J. N.; Hampson, R. F., Jr.; Hynes, R. G.; Jenkin, M. E.; Kerr, J. A.; Rossi, M. J.; Troe, J. Summary of evaluated kinetic and photochemical data for atmospheric chemistry; IUPAC Subcommittee on Gas Kinetic Data Evaluation for Atmospheric Chemistry; Vol. Web Version June 2006.
(65) FACSIMILE for Windows, Version 4.0.31; MCPA Software Ltd.
(66) Barnes, I.; Becker, K. H.; Fink, E. H.; Reimer, A.; Zabel, F.; Niki, H. *Chem. Phys. Lett.* **1985**, *115*, 1.
(67) Marechal, Y. *J. Chem. Phys.* **1987**, *87*, 6344.
(68) Hjorth, J.; Ottobrini, G.; Restelli, G. *J. Phys. Chem.* **1988**, *92*, 2669.
(69) Notholt, J.; Cappellani, F.; Roesdahl, H.; Restelli, G. *Spectrochim. Acta, Part A* **1991**, *47A*, 477.
(70) Shiau, B.-R.; Tso, T.-L. *Huaxue* **1994**, *52*, 133.
(71) Vander Auwera, J. V.; Didriche, K.; Perrin, A.; Keller, F., submitted 2007.
(72) Yarwood, G.; Niki, H.; Maker, P. D. *J. Phys. Chem.* **1991**, *95*, 4773.
(73) Burkart, M.; Schramm, B. *J. Mol. Spectrosc.* **2003**, *217*, 153.
(74) Pope, F. D.; Smith, C. A.; Ashfold, M. N. R.; Orr-Ewing, A. J. *Phys. Chem. Chem. Phys.* **2005**, *7*, 79.
(75) Co, D. T.; Hanisco, T. F.; Anderson, J. G.; Keutsch, F. N. *J. Phys. Chem. A* **2005**, *109*, 10675.
(76) Smith, C. A.; Pope, F. D.; Cronin, B.; Parkes, C. B.; Orr-Ewing, A. J. *J. Phys. Chem. A* **2006**, *110*, 11645.
(77) Frisch, M. J.; Trucks, G. W.; Schlegel, H. B.; Scuseria, G. E.; Robb, M. A.; Cheeseman, J. R.; Montgomery, J. A., Jr.; Vreven, T.; Kudin, K. N.; Burant, J. C.; Millam, J. M.; Iyengar, S. S.; Tomasi, J.; Barone, V.; Mennucci, B.; Cossi, M.; Scalmani, G.; Rega, N.; Petersson, G. A.; Nakatsuji, H.; Hada, M.; Ehara, M.; Toyota, K.; Fukuda, R.; Hasegawa, J.; Ishida, M.; Nakajima, T.; Honda, Y.; Kitao, O.; Nakai, H.; Klene, M.; Li, X.; Knox, J. E.; Hratchian, H. P.; Cross, J. B.; Bakken, V.; Adamo, C.; Jaramillo, J.; Gomperts, R.; Stratmann, R. E.; Yazyev, O.; Austin, A. J.; Cammi, R.; Pomelli, C.; Ochterski, J. W.; Ayala, P. Y.; Morokuma, K.; Voth, G. A.; Salvador, P.; Dannenberg, J. J.; Zakrzewski, V. G.; Dapprich, S.; Daniels, A. D.; Strain, M. C.; Farkas, O.; Malick, D. K.; Rabuck, A. D.; Raghavachari, K.; Foresman, J. B.; Ortiz, J. V.; Cui, Q.; Baboul, A. G.; Clifford, S.; Cioslowski, J.; Stefanov, B. B.; Liu, G.; Liashenko, A.; Piskorz, P.; Komaromi, I.; Martin, R. L.; Fox, D. J.; Keith, T.; Al-Laham, M. A.; Peng, C. Y.; Nanayakkara, A.; Challacombe, M.; Gill, P. M. W.; Johnson, B.; Chen, W.; Wong, M. W.; Gonzalez, C.; Pople, J. A. *Gaussian 03*, revision B.03; Gaussian, Inc.: Wallingford, CT, 2004.
(78) Orphal, J.; Chance, K. *J. Quant. Spectrosc. Radiat. Transfer* **2003**, *82*, 491.
(79) Rice, A. L.; Quay, P. D. *Anal. Chem.* **2006**, *78*, 6320.
(80) Yin, H. M.; Kable, S. H.; Zhang, X.; Bowman, J. M. *Science* **2006**, *311*, 1443.